Injectable, cryopreservable mesenchymal stromal cell-loaded microbeads for pro-angiogenic therapy: *in vitro* proof-of-concept

Biomedical Materials

PAPER

Injectable, cryopreservable mesenchymal stromal cell-loaded microbeads for pro-angiogenic therapy: *in vitro* proof-of-concept

Francesco K Touani[1,5], **Inès Hamouda**[1,2], **Nicolas Noiseux**[1,4], **Corinne Hoesli**[3], **Shant Der Sarkissian**[1,4] and **Sophie Lerouge**[1,2,*]

[1] Centre de Recherche du Centre Hospitalier de l'Université de Montréal (CRCHUM), Montreal, Canada
[2] Department of Mechanical Engineering, École de technologie supérieure (ÉTS), Montreal, Canada
[3] Department of Chemical Engineering, McGill University, Montreal, Canada
[4] Department of Surgery, Université de Montréal, Montréal, Canada
[5] Department of Pharmacology and Physiology, Université de Montréal, Montreal, Canada
[*] Author to whom any correspondence should be addressed.

E-mail: sophie.lerouge@etsmtl.ca

Keywords: microbeads hydrogel, human mesenchymal stromal cells, pro-angiogenic function, cryopreservation, pharmacological preconditioning, cell therapy

Supplementary material for this article is available online

OPEN ACCESS

RECEIVED
29 July 2024

REVISED
26 November 2024

ACCEPTED FOR PUBLICATION
5 December 2024

PUBLISHED
8 January 2025

Abstract

Despite their recognized potential for ischemic tissue repair, the clinical use of human mesenchymal stromal cells (hMSC) is limited by the poor viability of cells after injection and the variability of their paracrine function. In this study, we show how the choice of biomaterial scaffolds and the addition of cell preconditioning treatment can address these limitations and establish a proof-of-concept for cryopreservable hMSC-loaded microbeads. Injectable microbeads in chitosan, chitosan–gelatin, and alginate were produced using stirred emulsification to obtain a similar volume moment mean diameter (D[4,3] $\sim$ 500 μm). Cell viability was determined through live/dead assays, and vascular endothelial growth factor (VEGF) release was measured by ELISA. Proangiogenic function was studied by measuring the wound closure velocity of human umbilical vein endothelial cells (HUVEC) co-cultured with MSC-loaded microbeads. The effect of freeze–thawing on microbeads morphology, porosity, injectability and encapsulated MSC was also studied. hMSC-loaded chitosan-based microbeads were found to release 11-fold more VEGF than alginate microbeads ($p < 0.0001$) and chitosan–gelatin was chosen for further studies because it presented the best cell viability. Preconditioning with celastrol significantly enhanced the viability (1.12-fold) and VEGF release (1.40-fold) of MSC-loaded in chitosan–gelatin microbeads, as well as their proangiogenic paracrine function (1.2-fold; $p < 0.05$). In addition, preconditioning significantly enhanced the viability of hMSC after 1 and 3 d in low-serum medium after cryopreservation ($p < 0.05$). Cryopreserved hMSC-loaded microbeads maintained their mechanical properties, were easily injectable through a 23G needle, and kept their paracrine function, enhancing the proliferation and migration of scratched HUVEC. This study shows the advantage of chitosan as a scaffold material and concludes that chitosan–gelatin microbeads with celastrol-preconditioned cells form a promising off-the-shelf, cryopreservable allogenic MSC product. *In vivo* testing is required to confirm their potential in treating ischemic diseases or other clinical applications.

1. Introduction

Ischemic diseases, characterized by reduced blood supply to organs and tissues, represent a serious health condition that includes myocardial infarction, stroke, and peripheral artery diseases, such as critical limb ischemia [1, 2]. The therapeutic potential of human mesenchymal stromal cells (hMSCs) in these diseases is now well recognized, and several studies have demonstrated their ability to promote tissue repair and angiogenesis [3]. However, the clinical outcomes of hMSCs are still limited by challenges such as poor cell viability and retention as well as large variability in their paracrine function [4, 5].

Cell delivery through a hydrogel scaffold can protect cells and enhance their retention and paracrine functions in the target tissues. Several studies have explored cell encapsulation techniques for enhancing the viability, retention, and functional delivery of therapeutic cells [6, 7]. Microencapsulation offers a particularly promising approach to protect and sustain the functions of hMSCs [8, 9]. Compared with larger scaffolds, microbeads allow better diffusion of oxygen and nutrients to the encapsulated cells, which is required for survival and functional performance [10]. Microbeads also lead to a faster release of proangiogenic cytokines produced by cells [11]. Moreover, while a bulk hydrogel may form a physical barrier to vascularization, the microbead format allows a newly formed vascularized network to pass between the microbeads. Finally, this format can be used to create a storable and ready-to-use allogenic product of microencapsulated cells for easier clinical transfer.

Despite these potential advantages, to the best of our knowledge, microbead-form cellular products lack good viability, paracrine function, or easy clinical transferability. Alginate is the most common biomaterial for cell microencapsulation in the literature, thanks to its rapid gelation in contact with Ca^{2+} ions [12, 13]. However, alginate's poor cell-adhesive properties, non-biodegradability, and mechanical instability in the presence of chelators are strong limitations. Chitosan thermosensitive hydrogels are a good alternative for cell encapsulation and eventual release from the material [11, 14] because of their biodegradability, biocompatibility, porosity, and gentle temperature-dependent physical gelation without a crosslinker [15–17]. Because chitosan cell-adhesive properties are also limited, blending the polymer with extracellular matrix components, such as gelatin, can help increase the viability and paracrine function of the cells [18–20]. The impact of scaffold composition on the efficacy of MSC-laden products has not been extensively studied. Moreover, the feasibility of freeze/thawing must be confirmed, as this process may have an impact on cell viability, microbead morphology, and mechanical properties [12, 21, 22].

The main objective of this study was to develop an injectable, cryopreservable, hMSC-loaded product with optimized properties to enhance the proangiogenic potential of MSCs, a critical factor for promoting the revascularisation in ischemic tissues. We explored the use of chitosan (CH), chitosan–gelatin (CH–Gel), and alginate (ALG) as primary materials for microbead formation by stirred emulsification (SE) and investigated the impact of the material choice on the mechanical properties, morphology, injectability, survival, and functional proangiogenic efficacy of encapsulated hMSC. We demonstrate the advantages of chitosan-based scaffolds in terms of proangiogenic function and establish the proof of concept of cryopreservable CH–Gel microspheres. We also show the potential of cell preconditioning by celastrol, a natural compound extracted from the root of the medicinal plant Thunder God Vine, *triptergium wilfordii* [23, 24] to enhance the efficacy of this cellular product.

2. Material and methods

2.1. Material

Chitosan from shrimp shells (ChitoClear HQG 110, 43 010, Mw 150–250 kDa, 89% degree of deacetylation) was procured from Primex, Iceland. Chemical reagents including sodium phosphate monobasic (NaH_2PO_4), sodium phosphate dibasic (Na_2HPO_4), sodium alginate from brown algae (MKBZ4415V, Mw 12–40 kDa, viscosity 5.0–40.0 cps), gelatin porcine skin type A (G1880), bovine serum albumin (BSA 7.5% v/v, A8412), calcium carbonate ($CaCO_3$), and HEPES, were acquired from Sigma-Aldrich, Oakville, ON, Canada. Sodium hydrogen carbonate ($NaHCO_3$) was purchased from MP Biomedicals (Solon, OH, USA). Light mineral oil (Parafilm oil light, O-121-1), minimum essential medium alpha (aMEM) glutamax (1X), fetal bovine serum (FBS), hydrochloric acid (HCl), and Eosin Y were sourced from Thermo Fisher Scientific (ON, Canada). Nutristem XF medium and supplements were obtained from Biological Industries (Israel). Bone marrow hMSC and human umbilical vein endothelial cells (HUVECs) were procured from Lonza (ON, Canada) and Cell Applications (SD, US), respectively. Toluidine blue, Plasmalyte A (Baxter), and acetic acid (ACROS, CA) were also used in this study. Cell culture-treated T175 and T75 flasks were used for cell culture (Sarstedt, Germany). Cell culture insert with 0.4 μm PET track-etched membrane (Falcon, USA) were used for coculture experiments.

2.2. Hydrogel formulations

All solutions used for hydrogel preparation were autoclaved (15 min at 121 °C) and stored at 4 °C prior use, except when indicated.

2.2.1. Alginate

ALG hydrogels were prepared by mixing the sodium alginate solution (at 2.22%w/v in HEPES buffer) with

calcium carbonate suspension (0.05 g ml^{-1} in HEPES buffer) and aMEM supplemented with 10% BSA without cells. The ratio (%vol) of alginate, calcium carbonate, and medium was 90:5:5. The final concentration of alginate was 2% w/v. This suspension gels in contact with the acidified oil (see section 2.5).

2.2.2. Chitosan

CH hydrogel was obtained by mixing a) an acidic CH solution (at 2.67%w/v in 0.12 M hydrochloric acid) with b) a mixture of $NaHCO_3$ and phosphate buffer (PB, made from sodium dibasic and monobasic phosphate in milliQ water), and immediately after, with c) aMEM supplemented with 10% BSA (w/wo cells) [25]. The $NaHCO_3$/PB solution was sterilized using a 0.22 μm filter. The ratio (%vol) of the three solutions was 60:20:20 with final CH concentration 1.6%w/v, 0.01 M PB, and 0.075 M of $NaHCO_3$. This thermosensitive solution gels at 37 °C (see section 2.5).

2.2.3. Chitosan–gelatin

Chitosan–gelatin (CH–Gel) hydrogel was prepared following the same procedure as for CH hydrogels; CH and Gel were initially dissolved in a hydrochloric acid solution (0.12 M). The final concentration of gelatin was 2% w/v and chitosan 1.6%w/v.

2.3. Rheology

The rheological properties of the CH and CH–Gel solutions and final hydrogels were assessed using an MCR301 rheometer (Anton Paar, Germany) equipped with a 25 mm parallel-plate (1 mm gap size). The viscosity of the solutions as a function of temperature (10 °C–40 °C) was assessed in rotational mode at a constant shear (1 s^{-1}). Gelation kinetics of the hydrogels, just after mixing solutions *a,b,c* as described in section 2.2, were monitored by recording the evolution of the storage (G') and loss (G'') moduli within the viscoelastic range, in oscillatory mode at constant frequency (1 Hz) and deformation amplitude (1%) over a 10 h period. Initially, the temperature was set at 22 °C for 10 min to assess stability at room temperature (RT), then quickly raised to 37 °C to mimic an injection into warm oil for gelation. To prevent evaporation, a thin layer of low-viscosity paraffin oil was added to the sample prior to each oscillatory measurement. The rheological curves presented in the results section are representative data for each measurement and are not averaged values, unless specified. The supplementary information (figure S1) contains the curves of all the replicates.

2.4. Compression

The mechanical properties of each hydrogel were studied by unconfined compression tests using a MACH-1™ Micromechanical System (Biomomentum, Laval, Canada) equipped with a 100 N load cell. In brief, 300 μl of hydrogel, as described in section 2.2, was molded into cylinders (diameter of 8.6 mm and 7 mm in height) and underwent compression until reaching a nominal strain of 80% at a rate of 100% per minute. The nominal stress was calculated based on the applied force and initial cross-sectional area of the sample and then plotted as a function of the nominal strain. The elastic modulus was determined from the slope of the linear regression within 0%–20% of strain.

2.5. Microbeads fabrication

The microbeads were fabricated by adapting the procedures described by Alinejad *et al* [11] and Hoesli *et al* [26]. Briefly, the temperature, stirring rate, and stirring duration were optimized to generate microbeads of similar D[4,3] for all formulations. CH or CH–Gel formulations were added dropwise into preheated mineral oil at 37 °C in 100 ml spinner flasks (BellCo Glass Inc., USA) using an 18 G needle syringe, and stirred at rotation speeds of 700 and 500 rpm, respectively, for 3 min. The speed was then reduced to 200 rpm for 7 min to complete gelation and to avoid damaging the gelled beads. Afterwards, HEPES buffer was added, prior to centrifugation (1 min at 377*x g*), and the collected microbeads were washed with HEPES buffer.

ALG microbeads were obtained by injecting the alginate formulation (as prepared in section 2.2.1) in mineral oil at RT under stirring (400 rpm) for 3 min. Acidified mineral oil (0.22%$_{v/v}$ acetic acid mixed into the oil by vortexing shortly before the process) was then added to the mixture and stirred (200 rpm) for additional 7 min. Microbeads were collected following the same procedure as for the CH and CH–Gel microbeads.

2.6. Microbeads characterization

2.6.1. Size distribution

The size distribution and D[4,3] [27] of empty microbeads were determined. In brief, microbeads were stained by incubating overnight in a HEPES buffer solution containing 0.04% (v:v) of either eosin (5 g l^{-1}, for CH– and CH–Gel) or Toluidine Blue (5 g l^{-1}, for ALG) to induce image contrast. Two images of the microbeads at different locations were captured using an optical microscope at 6.3x magnification (Olympus, Canada), before analysis using the Cell Profiler™ software (version 3.19).

2.6.2. Injectability

Injectability tests were performed by injecting the prepared microbeads (3-fold dilution in HEPES) using a 23 G needle (internal diameter of 337 μm). The shape and morphology of the microbeads before

and after injection were imaged at four different locations under a brightfield microscope (40x magnification, Leica DM LB2). The percentage of damaged microbeads was quantified.

2.6.3. Mechanical characterization of microbeads

The mechanical properties of empty CH– and ALG-based microbeads were assessed in MilliQ water at RT using a MicroSquisher with SquisherJoy software (CellScale, Canada). Owing to the difference in the maximum force reached during testing, a 406 µm microbeam was employed for CH-based microbeads, while a 202 µm microbeam was used for ALG. Compression cycles consisted of 80% deformation over 60 s loading, followed by a 20 s hold phase and a 60 s recovery phase. The testing ceased upon bead rupture. The maximum compressive force and deformation at rupture were measured on individual microbeads ($n \geqslant 12$).

2.6.4. Microbeads structural network

The microbead structural network was qualitatively observed on histological slides using the Aperio ImageScope software (Leica Biosystems). Microbeads were washed with phosphate buffered saline (PBS) and fixed in 10% formalin for 5 min at RT prior to be embedded in Histogel™ (Thermo Scientific). The samples were then embedded in paraffin, sliced (4 µm), and stained with Hematoxylin and Eosin.

2.6.5. Gelatin release assessment

The release profile of gelatin from CH–Gel microbeads was evaluated by colorimetric test using the Pierce BCA protein assay kit (Thermo Fisher). In brief, 500 µl of microbead suspension was immersed in 2000 µl of PBS 1X in falcon tubes (Sarstedt CA) at 37 °C, or 4 °C for the control group. At predetermined time points (1 h, 4 h, 24 h, 3 and 7 d), a 100 µl of the medium was collected for gelatin release analysis and replaced with fresh PBS. Absorbance was measured at a wavelength of 562 nm using a spectrophotometer (VarioSkan Multimode, Thermofisher), and the gelatin concentration was determined from a calibration curve.

2.7. Cell bioactivity

2.7.1. Cell culture and encapsulation

Bone marrow-derived hMSCs were cultured in Nutristem medium (6600 cells cm^{-2}) supplemented with 0.6%(v/v) nutrient growth factor supplement in T175 flasks (Sarstedt, Germany) until 90% confluence. HUVECs were cultured in endothelial cell growth-2 medium (PromoCell® CA) supplemented with 0.4%(v/v) growth factor at a density of 9000 cells cm^{-2} in T75 flasks to the same level of confluence. These cells were detached using a trypsin-EDTA solution and centrifuged at 377 × *g* for 5 min (hMSCs) or 42 × *g* for 5 min (HUVECs). hMSCs suspension at 5 million cells ml^{-1} in aMEM supplemented with 10%BSA was prepared to obtain hydrogels loaded with 1 million cells ml^{-1} after preparation as described in 2.2. HUVEC were used for the wound healing tests (section 2.7.4).

2.7.2. Cell preconditioning

Cell preconditioning with celastrol was conducted as previously described [25]. Briefly, hMSCs were incubated 1 hour with celastrol at concentrations of 0.1 and 1 µM, and DMSO (0.1% v/v) as a vehicle in aMEM supplemented with 1% FBS. The cells were subsequently rinsed three times with aMEM containing 1% FBS and then incubated for an additional 4 h in complete aMEM media (10% FBS) prior to encapsulation in the hydrogel.

2.7.3. Cell viability

Cell viability was determined using a live/dead assay (Thermo Fisher, CA, USA) on days 0, 1, 4, and 7. The microbeads were incubated with 2 µM calcein and 5.5 µM ethidium homodimer in serum-free MEM for 45 min. Live and dead cells were visualized using an inverted fluorescence microscope at 50x magnification (Leica DM IRB). Cell quantification was performed using the ImageJ software.

2.7.4. Paracrine activity

The paracrine proangiogenic activity of cell-loaded microbeads was evaluated by measuring vascular endothelial growth factor (VEGF) release as well as by co-culturing them with a wounded layer of HUVEC (scratch test assay).

For VEFG release, microbeads were incubated in low-serum media and on days 4 and 7, VEGF was measured in the supernatant using the Quantikine ELISA Human VEGF Immunoassay (Bio-techne) according to the manufacturer's protocol.

For the coculture test, encapsulated hMSCs (preconditioned or not)) were first cultured for 4 d in complete media. Two days before coculture, HUVECs were seeded at 38 800 cells cm^{-2} in the bottom of 24 well plates (Corning™) and grown to 100% confluence in complete endothelial cell growth medium 2. The cross-shaped wounds (figure 5(D)) were created in each well using a 200 µl pipette tip. Concurrently, encapsulated hMSCs were suspended in the basal endothelial cell growth medium supplemented with 1%FBS at a 1:1 volume ratio. A volume of 200 µl of the microbead suspension was introduced into each Boyden Transwell (Falcon®) and 500 µl of the same medium was introduced into each Boyden Transwell and at the bottom of each well plate. The negative control consisted of HUVECs in low serum medium (1%FBS) with cell-free hydrogel in the Transwell,

Table 1. Freezing media composition (PLA = Plasmalyte; BSA = Bovine serum albumin).

Freezing media	PLA (% v/v)	aMEM (%v/v)	BSA (%v/v)	DMSO (%v/v)
aMEM + BSA	—	70	20	10
	—	85	5	10
PLA + BSA	70	—	20	10
	85	—	5	10

whereas the positive control was HUVECs in complete medium with cell-free hydrogel. Imaging was performed at various time points (0, 4, 8, 24, 32, and 48 h) using 40x magnification brightfield microscopy (Leica DM LB2) to assess the wound closure velocity.

2.7.5. Cryopreservation

The impact of different freezing media on the hMSC-loaded microbeads was investigated (table 1). We compared combinations of BSA with aMEM or plasmalyte (PLA), all supplemented with 10%$_{v/v}$ DMSO [28, 29]. Cell-loaded microbeads were suspended at a volume ratio of 1:3 (beads to freezing media) and stored in cryovials (Corning) for one day at −80 °C, followed by six days in liquid nitrogen. For thawing, the cryovials were placed in a 37 °C water bath for 2 min, then centrifuged twice at 377x*g* for 1 min. A 200 µl suspension of cell-loaded microbeads (in aMEM 10% FBS) was seeded in 24-well plates, before addition of 800 µl of the corresponding media. The cells were allowed to recover for 4 d under physiological conditions (37 °C with 5% CO_2), after which the medium was replaced with complete or low serum medium for three more days. Conditioned media was collected on day 7 (accumulation of day 4–7) to evaluate VEGF release, and cell viability was assessed on days 1 and 7. Non-cryopreserved MSC-loaded microbeads were used as controls.

2.8. Statistical analysis

All results are represented as the mean ± SEM, and the number of experimental replicates (N) and the total sample number within experiments (n) are indicated in each figure caption. Comparisons between groups were performed using Student's t-test or ANOVA followed by Tukey's multiple comparison post-hoc analysis using GraphPad Prism 9.5.1 software. Differences were considered significant for p values below 0.05. Kruskal–Wallis non-parametric statistical tests were performed on data that did not follow a Gaussian distribution or had significantly different variances.

3. Results and discussion

This study aimed to create an injectable, cryopreservable, hMSC-loaded product with good pro-angiogenic function, for the repair of ischemic tissue. We first optimized the stirring process to create microbeads of various compositions (CH, CH–Gel, and ALG) but with similar diameters and compared their ability to promote cell survival and proangiogenic paracrine function.

3.1. Rheological and mechanical characterization of CH-based hydrogels

As a first step, the influence of temperature on CH and CH–Gel hydrogels was characterized by rheology since the viscosity and gelation kinetic are crucial parameters for the fabrication of microbeads. We confirmed that both CH and CH–Gel formed thermosensitive hydrogels upon the addition of a weak base ((i.e. the PB- $NaHCO_3$ mixture), as shown by the rapid increase in their storage modulus when passing from RT to body temperature (figure 1(A)) in accordance with our previous studies [16]. As the viscosity of CH–Gel solution itself is highly temperature-sensitive (significantly more viscous than the CH solution at 10 °C but converging to similar values at $T > 27$ °C, see figure 1(B)), we studied the effect of preheating the CH–Gel on rheological properties of hydrogels and microbead morphology. Time-sweep at 37 °C, mimicking the injection in warm oil, showed that both hydrogels exhibited rapid gelation and comparable final storage moduli (8.8 kPa for CH and 6.9 kPa for CH–Gel at 10 h (figure 1(C)). Compression tests further confirmed the absence of significant differences in mechanical properties between the CH and CH–Gel hydrogels, both presenting a relatively linear behavior until 20% of deformation, with a young modulus of approximately 28 kPa (figure 1(D)). Preheating the CH–Gel to 37 °C resulted in a lower initial viscosity, easier injection into the stirrer, more rapid gelation, and more uniform beads (see later). Therefore, this method was used in all experiments.

3.2. Fabrication and characterization of the microbeads

Microbeads composed of ALG, CH, and CH–Gel were created using SE (figure 2(A)). Empty microbeads were first evaluated for size distribution, injectability, and mechanical properties. SE offers a balance of control, efficiency, and versatility, making it suitable for a wide range of applications including cell therapy. By adjusting the stirring rate, we successfully produced ALG, CH, and CH–Gel microbeads

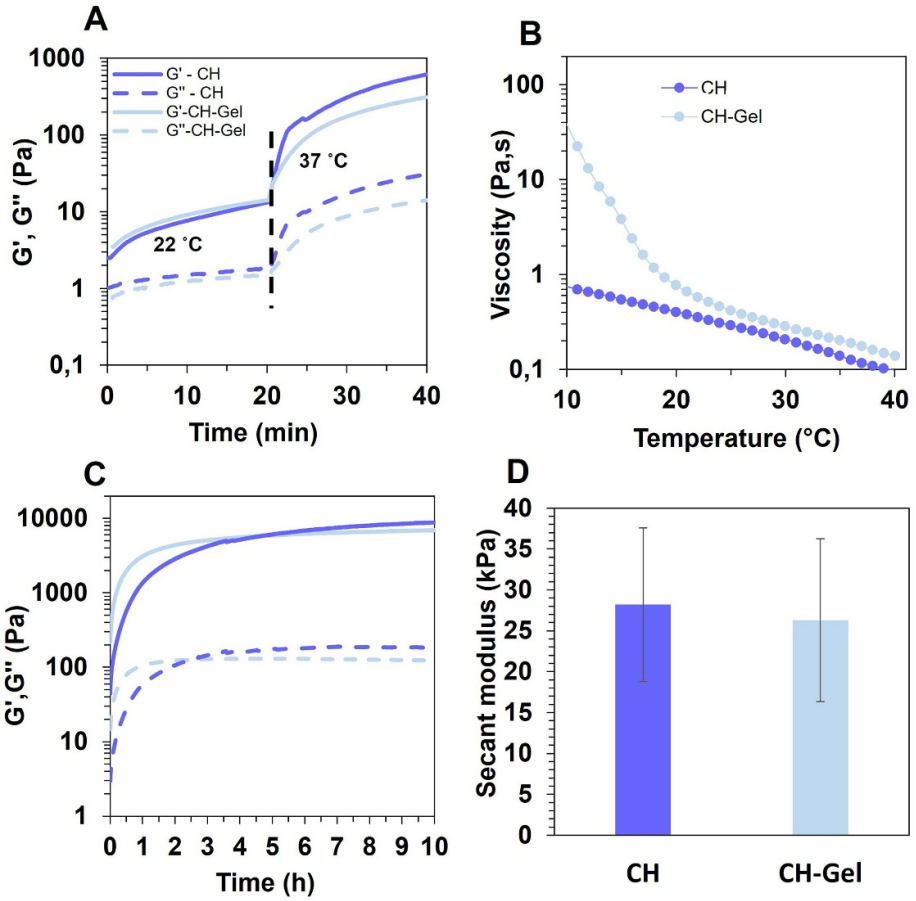

Figure 1. Rheological and mechanical characterization of CH and CH–Gel hydrogels: (A) thermosensitivity of hydrogels is demonstrated by rapid increase of the storage modulus G' when passing from 22 °C to 37 °C ($n = 6$) (G'' loss modulus); (B) viscosity (at a shear of 1 s^{-1}) of CH and CH–Gel acidic solutions as a function of temperature ($n = 3$); C) gelation kinetic at 37 °C when solutions had been preheated prior to mixing ($n = 6$).; (D) secant modulus at 20% of deformation after 24 h gelation ($n \geqslant 4$; $N \geqslant 3$).

with close D[4,3] (≈500 µm) [30] and size distribution (coefficients of variation of 37%, 35%, and 31%, respectively (figures 2(B)–(D)). As minimally invasive administration is important, we evaluated their injectability using 23G needles (figure 2(E)). ALG microbeads demonstrated a significantly higher rupture rate (30%) compared to CH and CH–Gel microbeads (10% and 12% respectively, $p < 0.01$).

Another advantage of these chitosan physical hydrogels for cell therapy is their interconnected porous structure owing to phase separation during gelation, as shown previously [31]. Since gelatin is a liquid at body temperature and could be partly released from the hydrogel, we evaluated gelatin release and the porosity of the microbeads after a 1 week incubation in PBS. As expected, gelatin release at 37 °C was significantly higher than at 4 °C (13 versus 6% at day 7, $p < 0.05$; figure 2(F)). This explains why microbeads incubated at 37 °C presented a higher porosity than microbeads incubated at 4 °C on histology, according to qualitative observations (figure 2(G) and S2).

The mechanical properties of the ALG, CH, CH–Gel, and cryopreserved CH–Gel microbeads (CH–Gel_Cryo) were further studied by compression tests using a Microsquisher (figure 3). ALG microbeads were more rigid but broke before reaching 40% deformation (figure 3(A)), consistent with the increased rupture rate obtained during injectability testing. In contrast, CH, CH–Gel, and CH–Gel_cryo (cryopreserved) microbeads underwent plastic deformation without breakage until 80% compression and resisted to drastically higher compression forces, demonstrating their superior mechanical strength (figures 3(B) and (C)). This was achieved thanks to the use of a specific mixture of $NaHCO_3$ and PB as gelling agents for CH-based gels, which was previously shown to drastically enhance their mechanical properties [17]. The mechanical properties of ALG microbeads can be enhanced by altering the molecular weight or crosslinking density using a higher guluronic/mannuronic (G/M) acid ratio [32]. However, a more rigid scaffold is not beneficial for encapsulated cells. The fragile rupture of ALG

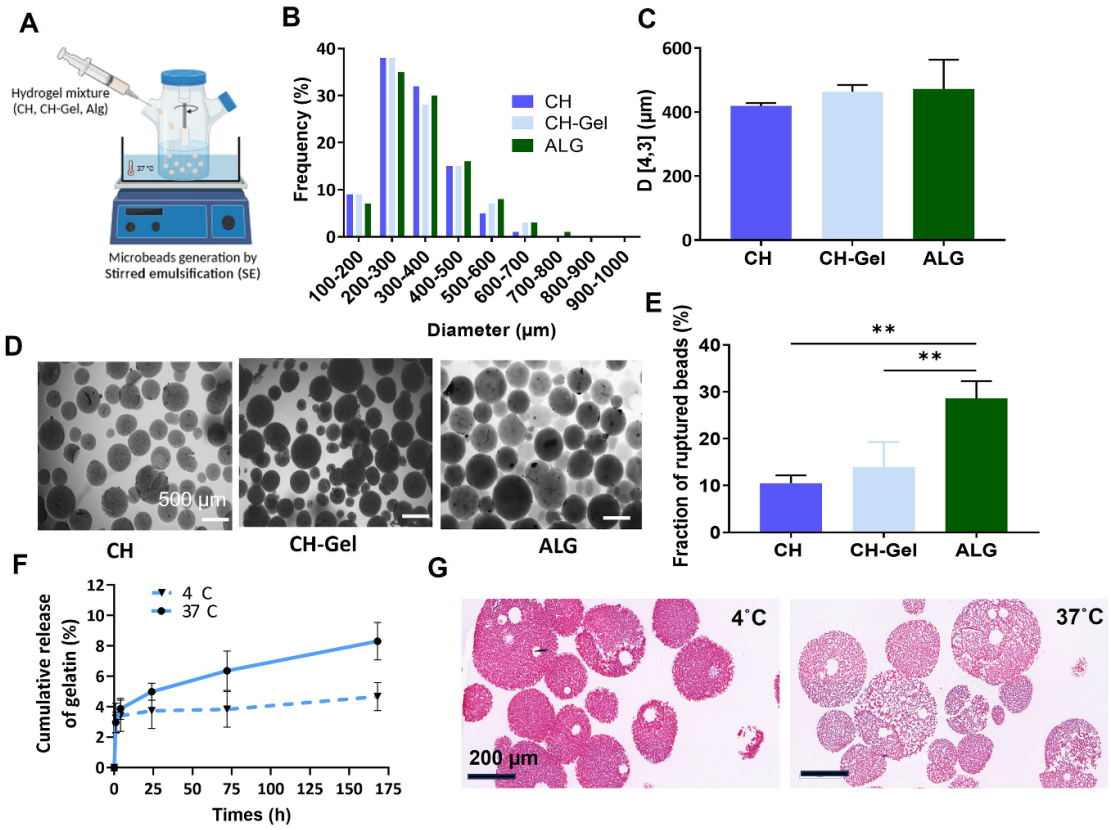

Figure 2. Microbead characterization and injectability: (A) schematic representation of microbeads fabrication with SE (with warm oil for CH and CH–Gel only); (B) size distribution and (C) volumic mean diameter D[4,3] ($n \geqslant 3000$ beads); (D) optical microscope images of empty CH, CH–Gel and ALG, microbeads (scale bar 500 µm); optimized stirring rates were 700, 500 and 400 rpm for CH, CH–Gel and ALG respectively; (E) percentage of ruptured empty microbeads after injection through a 23 G needle (mean ± SD; $n \geqslant 850$ beads; ** $P < 0.01$) (F) cumulative gelatin released from CH–Gel microbeads in PBS at 4 and 37 °C ($n = 4$); G) Microbeads structure after incubation at 37 °C and 4°C for 1 week (Histogel, H&E staining, 4 µm—thick histological sections); $N \geqslant 3$.

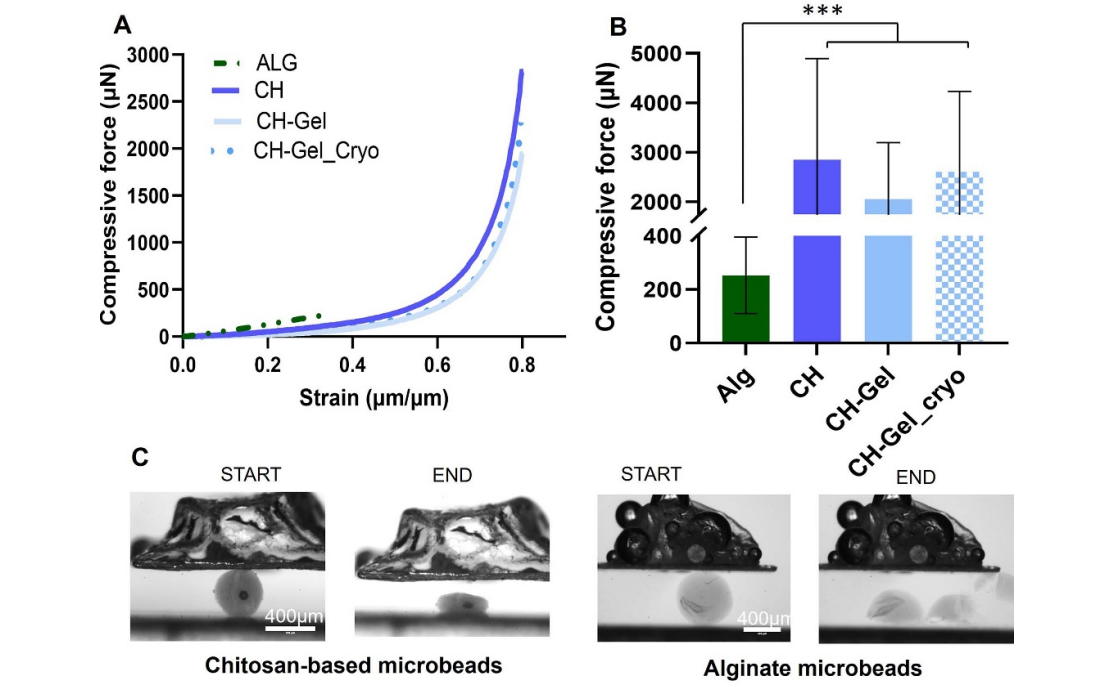

Figure 3. Mechanical properties of empty microbeads: (A) representative compression curves for alginate, chitosan, chitosan–gelatin and cryopreserved chitosan–gelatin microbeads, showing alginate breakage before 40% deformation while CH-based beads did not break until 80% deformation; (B) maximum compressive force (mean ± SD, $n \geqslant 10$, N = 2; *** $p < 0.001$); (C) representative images of chitosan and alginate microbeads before and after applying compression.

microbeads is a limitation compared to the plastic deformation of chitosan microbeads.

While 23G needles are considered adequate for most clinical applications [33], other teams have reported microbeads passing through smaller needles, such as 27G needles [34]. The diameter of the microbeads can be further reduced by increasing the stirring rate, decreasing the viscosity of the hydrogel solution, changing the impeller geometry, or adding an emulsifier [8, 35]. Other fabrication methods can also be proposed to reduce the size distribution [36] or avoid the use of oil [37].

3.3. Bioactivity of mesenchymal stromal cells-loaded microbeads

The viability of hMSCs encapsulated in CH, CH–Gel, and ALG microbeads was assessed in both complete (figure 4(A)) and low serum (figure 4(B)) culture media, revealing the highest viability in CH–Gel microbeads and the lowest in alginate under both conditions. After 7 days in complete media, CH–Gel, CH, and ALG microbeads exhibited cell viabilities of 80%, 70%, and 35%, respectively ($p < 0.05$). As expected, viability decreased under low serum conditions (66%, 55%, and 43%, respectively). Representative live/dead cell assay images are shown in figure 4(C).

These results are aligned with the study carried out by Cheng *et al* [18], demonstrating that blending gelatin 2 and 4% to chitosan scaffolds significantly enhances the viability of encapsulated adipose derived stromal cells (ASCs). The addition of gelatin can provide a more natural and supportive microenvironment for cells, providing cues that regulate cell behavior including adhesion,proliferation and migration. In addition, the increase in porosity of CH–Gel microbeads allows easier nutrient and oxygen access to the cell and increases their viability. Gelatin is an interesting material to enhance the efficacy of cell products owing to its biocompatibility, low immunogenicity, biodegradability, and ease of manipulation [38, 39].

Proangiogenic activity was evaluated by measuring VEGF release in low serum media over four days using ELISA (figure 4(D)). Drastically more VEGF (11-fold increase) was released from MSC-loaded CH and CH–Gel microbeads than from ALG microbeads (7461, 7431, and 670 pg ml^{-1} of hydrogel, respectively). This finding is crucial, as VEGF plays a vital role in angiogenesis, which is essential for ischemic tissue repair [40, 41].

The higher VEGF release from the chitosan-based scaffolds can be partly explained by the significantly lower cell viability observed in alginate, which can be related to several possible factors: its lower porosity, absence of cell-adhesive motifs [42, 43], shear stresses and traces of remaining oil from the SE process. However, cell viability decreased by less than two-fold, while VEGF release was approximately 11-fold, calling for additional explanations. To eliminate the possible effect of the remaining oil and shear during SE, which could influence cell viability and VEGF release, we confirmed the impact of the scaffold composition by encapsulating hMSC at the same concentration in bulk hydrogels of similar composition. Despite similar viability in the various hydrogels (77%, 74%, and 73% for CH–Gel, CH, and ALG, respectively) (see supplemental data S2), significantly higher VEGF release ($p<0.05$ was again observed from bulk CH–Gel and CH (11 737 and 16 816 pg ml^{-1} of hydrogel, respectively, $p = 0.9$.) compared to ALG (5057 pg ml^{-1} hydrogel, figure 4(E)).

These results highlight the importance of scaffold composition and suggest an advantage of CH-based scaffolds for cell therapy of ischemic diseases. The enhanced release of proangiogenic cytokines from chitosan scaffolds aligns with the existing literature, underscoring chitosan's effectiveness in neovascularization. Previous studies using bulk hydrogels have demonstrated that CH-based hydrogels enhance the proangiogenic potential of hMSCs through various mechanisms, including optimizing cell survival and engraftment, mitigating inflammatory responses, and promoting vascular endothelial stability, which collectively improve therapeutic outcomes in myocardial infarction and critical limb ischemia [18, 44, 45]. Moreover, a recent study showed the advantage of methacrylate glycol chitosan over methacrylate hyaluronic acid on proangiogenic (including VEGF) and immunomodulatory paracrine secretion by encapsulated ASC [46]. However, before conclusion, more extensive investigations are required, such as measuring other proangiogenic cytokines and characterizing the immunogenic response and reperfusion *in vivo* [47, 48]. The mode of cell death should be also assessed as cell necrosis might release intracellular molecules called alarmins which *in vivo* induce inflammation and cytokine storm [49].

Given the strong advantage of CH-based microbeads and bulk hydrogels over alginate in terms of VEGF release, and the significantly better cell viability in CH–Gel over CH in microbeads, CH–Gel was identified as the most promising formulation for subsequent experiments.

3.4. Effect of cell preconditioning by celastrol on the bioactivity of hMSC-loaded CH–Gel microbeads

To further improve cell viability and function in the CH–Gel microbeads, pharmacological cell preconditioning was performed prior to encapsulation by exposing the cells for 1 h to celastrol at 0.1 μM or 1 μM and to the vehicle (DMSO 0.1%) as a control (figure 5). Figure 5(A) shows the viability of encapsulated MSC on days 1 and 7. While cell viability was approximately 80% for all groups cultured

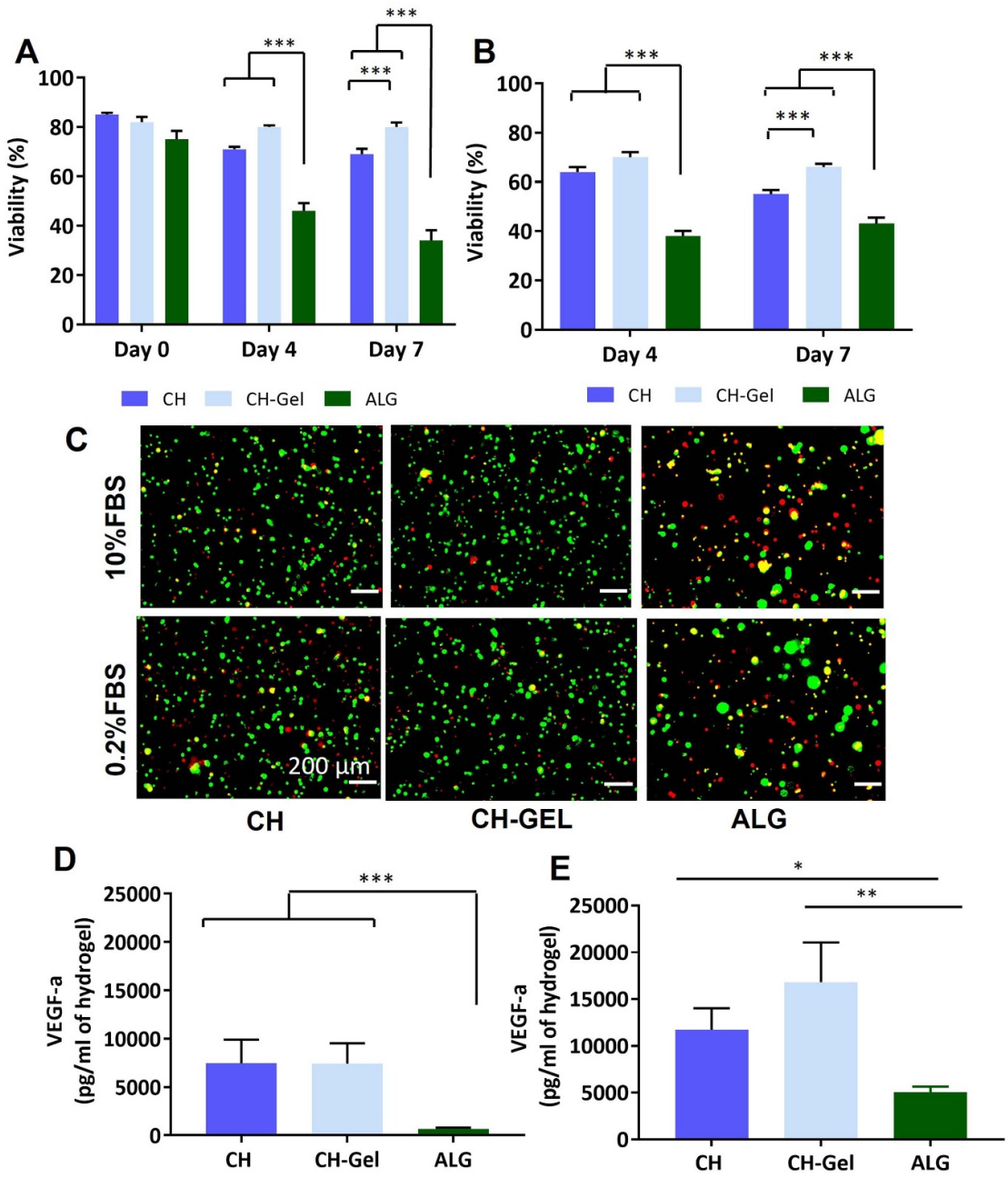

Figure 4. Viability of encapsulated hMSC cultured in (A) complete media (10%FBS) or (B) low serum media (0.2%FBS); (C) live/dead pictures at day 7; (D), (E) VEGF amount released at day 4 from MSC-loaded microbeads (D) and bulk hydrogels (E) ($n \geqslant 6$; $N \geqslant 2$; * $P < 0.05$, ** $P < 0.01$, *** $P < 0.001$).

in complete media, cell conditioning with celastrol 0.1 and 1 µM significantly increased the viability of cells cultured in low serum conditions by 10% and 12%, respectively ($p < 0.001$; figure 5(A)). In addition, VEGF released in the supernatant of preconditioned encapsulated cells increased by 25 and 40% for celastrol 0.1 and 1 µM, respectively, compared to the vehicle (figure 5(B)). The difference was only significant for celastrol at 1 µM ($p < 0.05$). These results corroborate our previous study, which demonstrated an increase in the viability and release of VEGF and SDF-1α proangiogenic cytokines from MSC pretreated with celastrol and loaded in bulk hydrogels, as well as their enhanced proangiogenic function *in vitro* and *in vivo* [25]. Preconditioning with celastrol seems particularly promising owing to its anti-inflammatory and pro-survival effects, which could be pivotal for increasing the viability and paracrine functions of hMSCs [23, 50]. Other teams have used sustained hypoxic preconditioning (1–3 days) prior to encapsulation to enhance the paracrine function of MSC [51, 52]. The advantage of our approach is the ease and short duration (1 h) of preconditioning treatment.

To confirm the proangiogenic paracrine function of the encapsulated hMSC, a scratched layer of

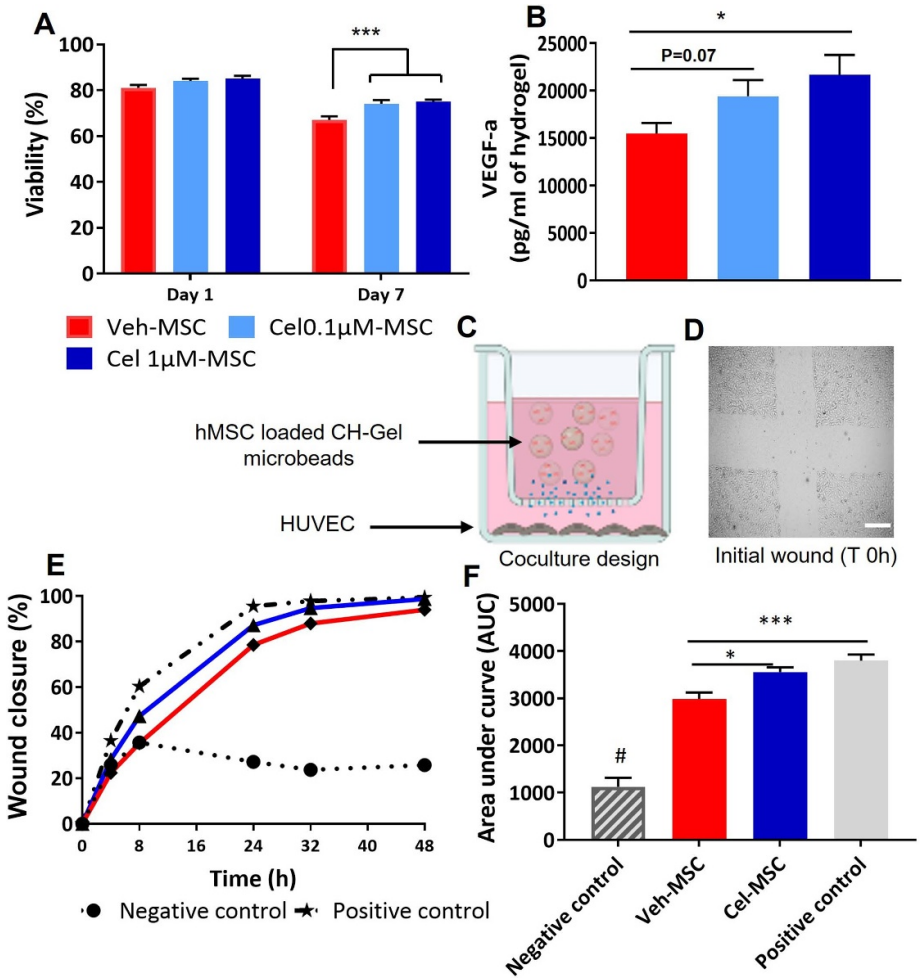

Figure 5. Effect of cell preconditioning by celastrol on the viability and VEGF release of hMSC loaded in CH–Gel microbeads: (A) cell viability at day 7 in complete and low serum culture media ($n \geqslant 6$); (B) VEGF released during day 4–7 ($n \geqslant 8$); (C) coculture model of MSC loaded microbeads and HUVEC; (D) initial wound at T0; (E) wound closure velocity with encapsulated hMSC preconditioned with celastrol 1 µM or vehicle, compared to positive control (empty microbeads in complete media) and negative control (empty microbead in low serum media); (F) area under the curve of wound closure ($n \geqslant 11$, $N \geqslant 3$). Results are expressed as mean ± SEM; $^{*}p < 0.05$; $^{***}P < 0.001$; # $P < 0.0001$ for negative control vs veh, cel and positive control.

HUVEC immersed in low serum media (1% FBS) was cocultured with microbeads loaded with hMSC pretreated with celastrol 1 µM) or vehicle (figures 5(C) and (D)). Cell-free microbeads in low serum (1% FBS) or complete endothelial cell growth medium-2 served as negative and positive controls, respectively. While there was no wound closure for the negative control, coculture of HUVEC with MSC-loaded microbeads (both vehicle- or celastrol-pretreated) led to rapid wound closure (figure 5(E)).

Wound closure was faster in cells preconditioned with celastrol (1 µM), which was also confirmed by a significant difference when analyzing the area under the curve (figure 5(F)). These results suggest that encapsulated cells have a good proangiogenic function, which was slightly increased by celastrol preconditioning. The combination of cell preconditioning and cell microencapsulation can be a promising strategy for improving the clinical outcomes of cell therapy, especially for ischemic tissue repair. Cell encapsulation can enhance cell retention and survival at target sites [53, 54].

3.5. Effect of cryopreservation on CH–Gel microbeads

For clinical transfer, it is essential to ensure that the cellular product can be stored until shipping and use in external clinical facilities. Therefore, we studied the feasibility of cryopreservation of hMSC-loaded microbeads.

First, we compared the effect of different freezing media compositions on the viability and VEGF release of encapsulated hMSC after cryopreservation. While the viability significantly decreased in all freezing media compared to fresh hMSC one day after thawing, we observed a good recovery of viability after one week of culture in complete media (figure 6(A)), with no significant difference from fresh cells. The best viability was obtained in PLA + BSA media (75 and 76% for PLA in 5 and 20% BSA, respectively)

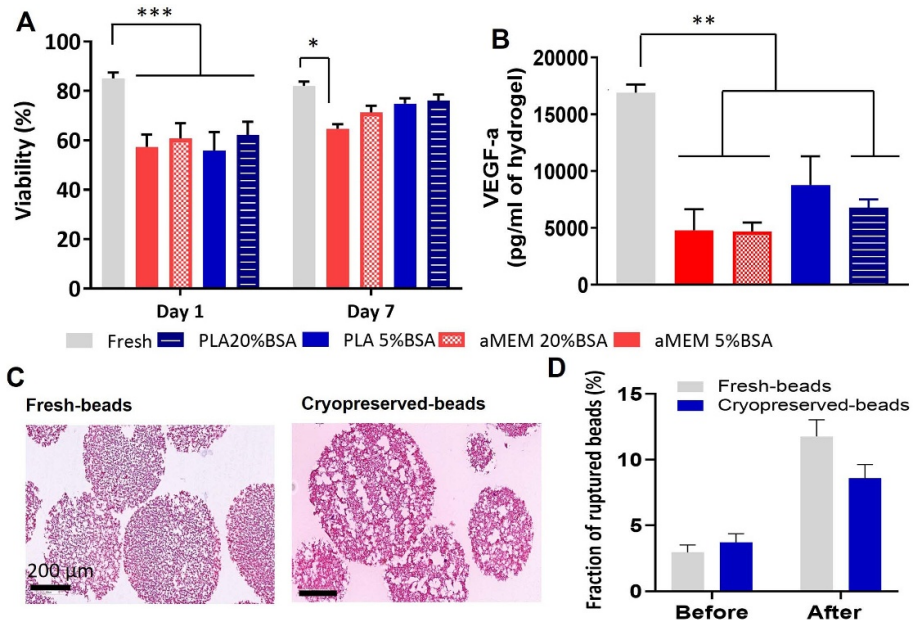

Figure 6. Effect of freezing media composition on the viability and bioactivity of microencapsulated MSC: (A) viability of encapsulated MSC, cryopreserved using different freezing media composition, 1 d and 1 week after thawing ($n \geqslant 4$, $N = 2$); (B) VEGF released within 3 d in low serum media (days 4–7)($n \geqslant 3$, $N = 2$); (C) structure of cryopreserved microbeads after 7 d of culture; (D) injectability of MSC-loaded fresh and cryopreserved microbeads through 23G needle ($n \geqslant 6$). Control is non-injected microbeads. * $P < 0.05$; ** $P < 0.01$; *** $p < 0.001$. PLA = Plasmalyte A, BSA = Bovine serum albumin.

with DMSO choose as permeating cryoprotectant (CPA). This is a bit lower than the 80% viability reported for non-encapsulated cells in the PLA + BSA cryopreservation media [28, 29]. The difference could be due to reduced infiltration of the media within the cells during freezing due to the hydrogel microbeads [22].

Cryopreservation also decreased VEGF release, the difference with fresh MSC-loaded beads was significant, except with PLA + 5%BSA freezing media ($p = 0.14$) (figure 6(B)), which was maintained for further experiments. CH–Gel microbeads cryopreserved in PLA + 5%BSA were stable, maintained their structure after one week of culture, and showed increased porosity compared to fresh microbeads (figure 6(C)). They were still injectable through a 23 G needle with only 8% ruptured beads versus 12% for fresh beads (figure 6(D)). As shown in previous figure 3(B), cryopreservation did also not alter the mechanical properties of the microbeads, which presented similar compressive strength and no rupture until 80% of compression.

More importantly, a functional assay of wounded HUVEC (figures 7(B) and (C)) confirmed the proangiogenic paracrine activity of microencapsulated freeze-thawed cells, and significant wound closure was obtained within 24 h, while HUVEC subjected only to the low serum media did not proliferate and close the wound. The rate of closure was very close to that of freshly encapsulated MSC (figure 7(D)).

While preconditioning with Celastrol 0.1 µM helped increase the cell viability immediately after freeze–thawing microbeads (66% vs. 55% for vehicle, $p < 0.01$) and after 3 d in low-serum media (72 vs. 65%, $p<0.05$; figure 7(A)), no further benefit was detected during wound closure tests.

These results confirmed the feasibility of cryopreservation of MSC-loaded CH-based microbeads. The best results were obtained with freezing media made from Plasmalyte A, serum albumin (SA), and DMSO. This type of medium is increasingly used for clinical purposes, where FBS must be avoided owing to immunological responses [29, 55]. In the cryopreservation process, SA helps stabilize the cell membranes and maintain the osmolarity and pH of the cryopreservation solution [56] In clinical studies, bovine SA are replaced by human SA. Cryopreservation can be further improved by optimizing the choice of CPA using permeating CPA (DMSO, glycerol), non-permeating CPA (sugars such as sucrose and trehalose), or a combination of permeating/non-permeating CPA [57, 58]. It can also be optimized by adding antioxidant stabilizers [59] and ice nucleating agents [60] to freezing media.

3.6. Chitosan-gel microbeads, a promising cell therapy product

In this study, we showed that chitosan has several advantages over alginate for cell encapsulation and injection *in vitro*.

Alginate-based microbeads are most commonly used for *in vitro* culture and storage [12, 58, 61] because of the ease of microbead fabrication and the ability to reverse ionic crosslinking when immersing the gel in a chelating solution [62] but they are far from ideal for cell therapy. Their limitations

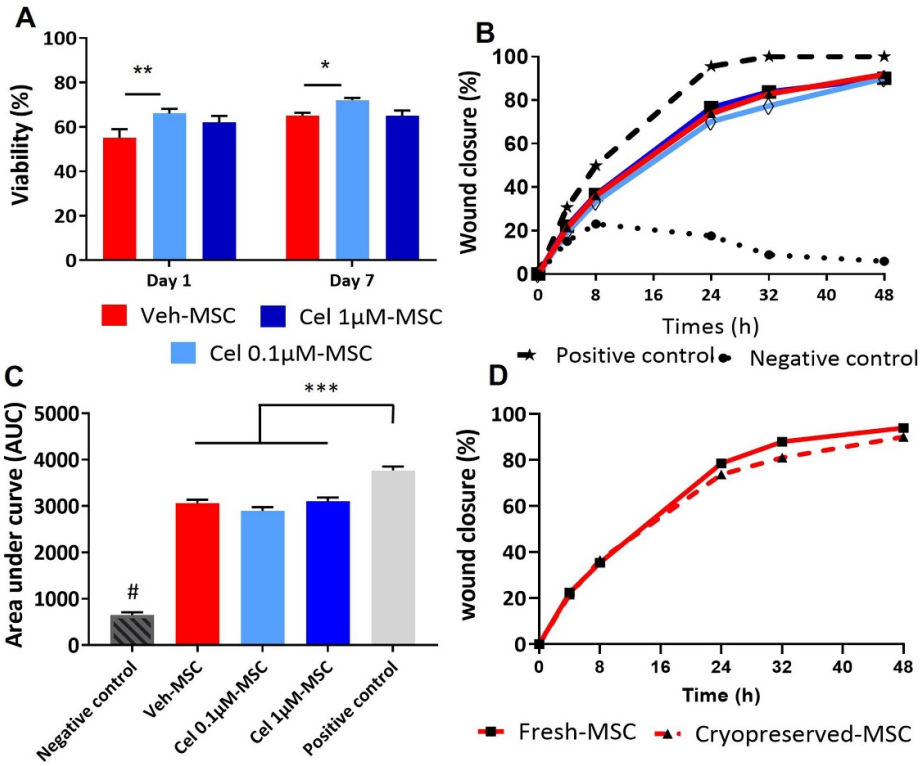

Figure 7. Effect of cryopreservation and cell preconditioning on paracrine activity of MSC-loaded CH–Gel microbeads. (A) Viability at day1 and 7 in cryopreserved microbeads, preconditioned with celastrol 0.1, 1 µM or vehicle, cultured in 10%FBS or 0.2%FBS (4 d in 10%FBS and 3 d 0.2%FBS) ($n \geqslant 6$; $N \geqslant 2$); (B) wound closure velocity of HUVEC cocultured with cryopreserved CH–Gel beads loaded with hMSC preconditioned with celastrol 0.1, 1 µM or vehicle; (C) area under the curve of wound closure (mean ± SEM;$n \geqslant 7$,$n = 2$); (D) wound closure velocity with fresh versus freeze/thawed hMSC loaded microbeads ($n \geqslant 14$ $N \geqslant 2$) insert: area under the curve. * $P < 0.05$; ** $P < 0.01$; *** $P < 0.001$; # $P < 0.0001$ negative control vs all other groups.

include the lack of cell adhesive motifs, lack of stability in various physiological solutions used in clinics [62, 63], and the absence of biodegradation. Other materials have been proposed for the formation of cryopreservable MSC-loaded microbeads with good cell viability, for instance polyD,L-lactic-co-glycolic acid (PLGA)[64] PLGA is biodegradable. However, its degradation products (lactic and glycolic acids) can cause localized acidic environments and generate inflammation.

Compared with these materials, CH–Gel microbeads form a particularly promising alternative for cell therapy. They are easy to prepare and require no chemical modification or toxic crosslinkers. They are biodegradable and easily injectable using small needles. They can support MSC viability and paracrine function, are stable in various physiological solutions, and can be cryopreserved.

4. Conclusion

In this study, we established the *in vitro* proof-of-concept for cryopreservable hMSC-encapsulated CH–Gel microbeads as an injectable system to promote revascularisation of ischemic tissues. The drastic increase in VEGF release from hMSC-loaded CH and CH–Gel microbeads compared to ALG highlights the importance of scaffold composition on the efficacy of cell therapy products. Owing to its better cell viability compared to CH, CH–Gel was selected as the most promising formulation. The CH–Gel microbeads formed by SE exhibit good porosity, injectability, stability, and mechanical properties with ductile behavior under load, which prevents fragile rupture. Such a microbead format is particularly appealing as it allows vascularization throughout the implanted bead network, whereas bulk hydrogels may act as a barrier to reperfusion when injected into the ischemic region [10]. In addition, microbeads allow easier access of O_2 and nutrients to cells. Its combination with cell preconditioning, by simple exposure of the cells for 1 h to celastrol prior to encapsulation, further enhanced the survival of encapsulated cells and the proangiogenic function of this cellular product. Finally, its cryopreservability was demonstrated using a mixture of Plasmalyte, serum albumin, and DMSO as the freezing media. This is a promising off-the-shelf, cryopreserved allogenic MSC product with good viability and paracrine function for the minimally invasive treatment of ischemic diseases. Its bioactivity could be further enhanced by optimizing the preconditioning treatment or freeze–thawing method. Moreover, understanding the mechanisms underlying the enhanced efficacy of CH–Gel scaffolds and celastrol-preconditioned MSCs and more importantly, testing in animal models is required to validate their clinical potential.

Data availability statement

All data that support the findings of this study are included within the article (and any supplementary files).

Author contributions

Francesco Touani Kameni: Investigation, Conceptualization, Methodology, Data acquisition and analysis, original draft, writing, review, and editing. **Inès Hamouda**: Methodology, Data analysis, original draft, writing, review, and editing. **Corinne Hoesli**: methodology and review editing. **Nicolas Noiseux:** review and editing. **Shant Der Sarkissian:** Conceptualization, Methodology, Data analysis, writing review, and editing. **Sophie Lerouge**: Conceptualization, Methodology, Data analysis, original draft, writing–review and editing, project administration resources, and funding acquisition.

Acknowledgment

This study was funded by the Quebec Cell, Tissue and Gene Therapy Network–ThéCell (a thematic support network by the FRQ-S), FRQNT team project, and NSERC (RGPIN2020-06884). We also thank Mr. Yohan Vigouroux and Mrs. Melanie Borie for their technical help with this project.

Conflict of interest

The authors declare that they have no conflicts of interest.

ORCID iDs

Francesco K Touani https://orcid.org/0000-0002-3976-2438
Shant Der Sarkissian https://orcid.org/0000-0002-5666-3546
Sophie Lerouge https://orcid.org/0000-0002-4992-5552

References

[1] Man S, Xian Y, Holmes D N, Matsouaka R A, Saver J L, Smith E E, Bhatt D L, Schwamm L H and Fonarow G C 2020 Association between thrombolytic door-to-needle time and 1-year mortality and readmission in patients with acute ischemic stroke *JAMA* **323** 2170–84
[2] Hirsch A T, Haskal Z J, Hertzer N R, Bakal C W, Creager M A, Halperin J L and White R A 2006 ACC/AHA 2005 practice guidelines for the management of patients with peripheral arterial disease (lower extremity, renal, mesenteric, and abdominal aortic) *Circulation* **113** e463–654
[3] Parikh P P, Liu Z J and Velazquez O C 2017 A molecular and clinical review of stem cell therapy in critical limb ischemia *Stem Cells Int.* **2017** 3750829
[4] Wong J K U, Mehta A, Vũ T T and Yeo G C 2023 Cellular modifications and biomaterial design to improve mesenchymal stem cell transplantation *Biomater. Sci.* **11** 4752–73
[5] Elshaer S L, Bahram S H, Rajashekar P, Gangaraju R and El-Remessy A B 2021 Modulation of mesenchymal stem cells for enhanced therapeutic utility in ischemic vascular diseases *Int. J. Mol. Sci.* **23** 249
[6] Roche E T, Hastings C L, Lewin S A, Shvartsman D E, Brudno Y, Vasilyev N V, O'Brien F J, Walsh C J, Duffy G P and Mooney D J 2014 Comparison of biomaterial delivery vehicles for improving acute retention of stem cells in the infarcted heart *Biomaterials* **35** 6850–8
[7] Rustad K C, Wong V W, Sorkin M, Glotzbach J P, Major M R, Rajadas J, Longaker M T and Gurtner G C 2012 Enhancement of mesenchymal stem cell angiogenic capacity and stemness by a biomimetic hydrogel scaffold *Biomaterials* **33** 80–90
[8] Lee S-Y, Ma J, Khoo T S, Abdullah N, Nik Md Noordin Kahar N N F, Abdul Hamid Z A and Mustapha M 2021 Polysaccharide-based hydrogels for microencapsulation of stem cells in regenerative medicine *Front. Bioeng. Biotechnol.* **9** 735090
[9] Yao R, Zhang R, Luan J and Lin F 2012 Alginate and alginate/gelatin microspheres for human adipose-derived stem cell encapsulation and differentiation *Biofabrication* **4** 025007
[10] Qazi T H and Burdick J A 2021 Granular hydrogels for endogenous tissue repair *Biomater. Biosyst.* **1** 100008
[11] Alinejad Y, Bitar C M, Martinez Villegas K, Perignon S, Hoesli C A and Lerouge S 2020 Chitosan microbeads produced by a one-step scalable stirred emulsification: a promising process for cell therapy applications *ACS Biomater. Sci. Eng.* **6** 288–97
[12] Pravdyuk A I, Petrenko Y A, Fuller B J and Petrenko A Y 2013 Cryopreservation of alginate encapsulated mesenchymal stromal cells *Cryobiology* **66** 215–22
[13] Haque T, Chen H, Ouyang W, Martoni C, Lawuyi B, Urbanska A M and Prakash S 2005 *In vitro* study of alginate-chitosan microcapsules: an alternative to liver cell transplants for the treatment of liver failure *Biotechnol. Lett.* **27** 317–22
[14] Tao Y, Zhang H-L, Hu Y-M, Wan S and Su Z-Q 2013 Preparation of chitosan and water-soluble chitosan microspheres via spray-drying method to lower blood lipids in rats fed with high-fat diets *Int. J. Mol. Sci.* **14** 4174–84
[15] Chenite A C, Chaput C, Wang D, Combes C, Buschmann M D, Hoemann C D, Leroux J C, Atkinson B L, Binette F and Selmani A 2000 Novel injectable neutral solutions of chitosan form biodegradable gels *in situ* *Biomaterials* **21** 2155–61
[16] Ceccaldi C, Assaad E, Hui E, Buccionyte M, Adoungotchodo A and Lerouge S 2017 Optimization of injectable thermosensitive scaffolds with enhanced mechanical properties for cell therapy *Macromol. Biosci.* **17** 1600435
[17] Assaad E, Maire M and Lerouge S 2015 Injectable thermosensitive chitosan hydrogels with controlled gelation kinetics and enhanced mechanical resistance *Carbohydrate Polym.* **130** 87–96
[18] Cheng N C, Lin W J, Ling T Y and Young T H 2017 Sustained release of adipose-derived stem cells by thermosensitive chitosan/gelatin hydrogel for therapeutic angiogenesis *Acta Biomater.* **51** 258–67
[19] Hosaka A, Koyama H, Kushibiki T, Tabata Y, Nishiyama N, Miyata T, Shigematsu H, Takato T and Nagawa H 2004 Gelatin hydrogel microspheres enable pinpoint delivery of basic fibroblast growth factor for the development of functional collateral vessels *Circulation* **110** 3322–8
[20] Georgopoulou A, Papadogiannis F, Batsali A, Marakis J, Alpantaki K, Eliopoulos A G, Pontikoglou C and Chatzinikolaidou M 2018 Chitosan/gelatin scaffolds support bone regeneration *J. Mater. Sci., Mater. Med.* **29** 59
[21] Rogulska O, Tykhvynska O, Revenko O, Grischuk V, Mazur S, Volkova N, Vasyliev R, Petrenko A and Petrenko Y 2019 Novel cryopreservation approach providing off-the-shelf availability of human multipotent mesenchymal stromal

cells for clinical applications *Stem Cells Int.* **2019** 4150690
[22] Zhang C, Zhou Y, Zhang L, Wu L, Chen Y, Xie D and Chen W 2018 Hydrogel cryopreservation system: an effective method for cell storage *Int. J. Mol. Sci.* **19** 3330
[23] Der Sarkissian S, Cailhier J-F, Borie M, Stevens L-M, Gaboury L, Mansour S, Hamet P and Noiseux N 2014 Celastrol protects ischaemic myocardium through a heat shock response with up-regulation of haeme oxygenase-1 *Br. J. Pharmacol.* **171** 5265–79
[24] Aceros H, Der Sarkissian S, Borie M, Stevens L M, Mansour S and Noiseux N 2019 Celastrol-type HSP90 modulators allow for potent cardioprotective effects *Life Sci.* **227** 8–19
[25] Touani F K, Borie M, Azzi F, Trudel D, Noiseux N, Der Sarkissian S and Lerouge S 2021 Pharmacological preconditioning improves the viability and proangiogenic paracrine function of hydrogel-encapsulated mesenchymal stromal cells *Stem Cells Int.* **2021** 6663467
[26] Hoesli C A, Raghuram K, Kiang R L J, Mocinecova D, Hu X, Johnson J D, Lacík I, Kieffer T J and Piret J M 2011 Pancreatic cell immobilization in alginate beads produced by emulsion and internal gelation *Biotechnol. Bioeng.* **108** 424–34
[27] Ebert S, Grossmann L, Hinrichs J and Weiss J 2019 Emulsifying properties of water-soluble proteins extracted from the microalgae chlorella sorokiniana and phaeodactylum tricornutum *Food Funct.* **10** 754–64
[28] Pollock K, Sumstad D, Kadidlo D, McKenna D H and Hubel A 2015 Clinical mesenchymal stromal cell products undergo functional changes in response to freezing *Cytotherapy* **17** 38–45
[29] Kaplan A, Sackett K, Sumstad D, Kadidlo D and McKenna D H 2017 Impact of starting material (fresh versus cryopreserved marrow) on mesenchymal stem cell culture *Transfusion* **57** 2216–9
[30] Zhang X, Wang H and Luo L 2022 Comparison analysis of the calculation methods for particle diameter *Crystals* **12** 1107
[31] Bao G, Jiang T, Ravanbakhsh H, Reyes A, Ma Z, Strong M, Wang H, Kinsella J M, Li J and Mongeau L 2020 Triggered micropore-forming bioprinting of porous viscoelastic hydrogels *Mater. Horiz.* **7** 2336–47
[32] Bennacef C, Desobry S, Jasniewski J, Leclerc S, Probst L and Desobry-Banon S 2023 Influence of alginate properties and calcium chloride concentration on alginate bead reticulation and size: a phenomenological approach *Polymers* **15** 4163
[33] Songür N, Songür Y, Bırcan S and Kapucuoğlu N 2011 Comparison of 19-and 22-gauge needles in EUS-guided fine needle aspiration in patients with mediastinal masses and lymph nodes *Turk. J. Gastroenterol.* **22** 472–8
[34] Seong Y J, Lin G, Kim B J, Kim H E, Kim S and Jeong S H 2019 Hyaluronic acid-based hybrid hydrogel microspheres with enhanced structural stability and high injectability *ACS Omega* **4** 13834–44
[35] Wang L, Rao R R and Stegemann J P 2013 Delivery of mesenchymal stem cells in chitosan/collagen microbeads for orthopedic tissue repair *Cells Tissues Organs* **197** 333–43
[36] Shin D S, Touani F K, Aboud D G K, Kietzig A-M, Lerouge S and Hoesli C A 2023 Mammalian cell encapsulation in monodisperse chitosan beads using microchannel emulsification *Colloids Surf.* A **661** 130807
[37] Opara E C 2017 Methods in molecular biology *Cell Microencapsulation: Methods and Protocols* vol 1479 (Springer) p 336
[38] Dong Z, Meng X, Yang W, Zhang J, Sun P, Zhang H, Fang X, Wang D-A and Fan C 2021 Progress of gelatin-based microspheres (GMSs) as delivery vehicles of drug and cell *Mater. Sci. Eng.* C **122** 111949
[39] Fu J, Fan C, Lai W S and Wang D 2016 Enhancing vascularization of a gelatin-based micro-cavitary hydrogel by increasing the density of the micro-cavities *J. Biomed. Mater. Res.* **11** 055012
[40] Yong K W, Choi J R, Mohammadi M, Mitha A P, Sanati-Nezhad A and Sen A 2018 Mesenchymal stem cell therapy for ischemic tissues *Stem Cells Int.* **2018** 1–11
[41] Merckx G, Hosseinkhani B, Kuypers S, Deville S, Irobi J, Nelissen I, Michiels L, Lambrichts I and Bronckaers A 2020 Angiogenic effects of human dental pulp and bone marrow-derived mesenchymal stromal cells and their extracellular vesicles *Cells* **9** 312
[42] Sarker B, Rompf J, Silva R, Lang N, Detsch R, Kaschta J, Fabry B and Boccaccini A R 2015 Alginate-based hydrogels with improved adhesive properties for cell encapsulation *Int. J. Biol. Macromol.* **78** 72–78
[43] Silva J M, Garcia J R, Reis R L, Garcia A J and Mano J F 2017 Tuning cell adhesive properties via layer-by-layer assembly of chitosan and alginate *Acta Biomater.* **51** 279–93
[44] Hastings C L, Kelly H M, Murphy M J, Barry F P, O'Brien F J and Duffy G P 2012 Development of a thermoresponsive chitosan gel combined with human mesenchymal stem cells and desferrioxamine as a multimodal pro-angiogenic therapeutic for the treatment of critical limb ischaemia *J. Control. Release Soc.* **161** 73–80
[45] Zhao N *et al* 2019 IGF-1C domain-modified hydrogel enhances therapeutic potential of mesenchymal stem cells for hindlimb ischemia *Stem Cell Res. Ther.* **10** 129
[46] Serack F E 2023 *Development of a Cell-based Regenerative Strategy to Modulate Angiogenesis and Inflammation in Ischemic Muscle* (University of Western Ontario)
[47] Sareen N, Srivastava A and Dhingra S 2021 Role of prostaglandin E2 in allogeneic mesenchymal stem cell therapy for cardiac repair *Can. J. Physiol. Pharmacol.* **99** 140–50
[48] Dhingra S, Huang X-P and Li R-K 2010 Challenges in allogeneic mesenchymal stem cell–mediated cardiac repair *Trend Cardiovasc. Med.* **20** 263–8
[49] Karki R and Kanneganti T D 2021 The 'cytokine storm': molecular mechanisms and therapeutic prospects *Trends Immunol.* **42** 681–705
[50] Aceros H, Der Sarkissian S, Borie M, Ribeiro R V P, Stevens L-M, Maltais S, Stevens L M and Noiseux N 2020 Novel heat shock protein 90 inhibitor improves cardiac recovery in a rodent model of donation after circulatory death *J. Thoracic Cardiovasc. Surg.* **163** e187–e197
[51] Naderi-Meshkin H *et al* 2016 Injectable hydrogel delivery plus preconditioning of mesenchymal stem cells: exploitation of SDF-1/CXCR4 axis toward enhancing the efficacy of stem cells' homing *Cell Biol. Int. Rep.* **40** 730–41
[52] Tong C, Hao H, Xia L, Liu J, Ti D, Dong L and Han W 2016 Hypoxia pretreatment of bone marrow-derived mesenchymal stem cells seeded in a collagen-chitosan sponge scaffold promotes skin wound healing in diabetic rats with hindlimb ischemia *Wound Repair Regener.* **24** 45–56
[53] Huang Y, Li X and Yang L 2022 Hydrogel encapsulation: taking the therapy of mesenchymal stem cells and their derived secretome to the next level *Front. Bioeng. Biotechnol.* **10** 859927
[54] Young S A, Sherman S E, Cooper T T, Brown C, Anjum F and Hess D A 2015 A mechanically robust injectable hydrogel scaffold for adipose-derived stem cell delivery for the treatment of peripheral arterial disease *Tissue Eng. A* **159** 146–60
[55] Pal R, Hanwate M and Totey S M 2008 Effect of holding time, temperature and different parenteral solutions on viability and functionality of adult bone marrow-derived mesenchymal stem cells before transplantation *J. Tissue Eng. Regener. Med.* **2** 436–44
[56] Volkova N, Yukhta M, Sokil L, Chernyschenko L, Stepanyuk L and Goltsev A 2021 Application efficiency of bovine serum albumin for recovery of seminiferous tubules of testes after cryopreservation *Biotechnol. Acta* **14** 28–36
[57] Gurruchaga H, Saenz Del Burgo L, Hernandez R M, Orive G, Selden C, Fuller B, Ciriza J and Pedraz J L 2018 Advances in the slow freezing cryopreservation of microencapsulated cells *J. Control. Release* **281** 119–38

[58] Cui Y, Nash A M, Castillo B, Sanchez Solis L D, Aghlara-Fotovat S, Levitan M, Kim B, Diehl M and Veiseh O 2022 Development of serum-free media for cryopreservation of hydrogel encapsulated cell-based therapeutics *Cell Mol. Bioeng.* **15** 425–37
[59] Limaye L and Kale V 2001 Cryopreservation of human hematopoietic cells with membrane stabilizers and bioantioxidants as additives in the conventional freezing medium *J. Hematotherapy Stem Cell Res.* **10** 709–18
[60] Morris G J and Acton E 2013 Controlled ice nucleation in cryopreservation–a review *Cryobiology* **66** 85–92
[61] Nurhayati R W, Pratama G and Dinastri M (ed) 2022 The cryoprotecting effects of trehalose and dimethyl sulfoxide on alginate-chitosan encapsulated mesenchymal stem cells *AIP Conf. Proc.* **2537** 020006
[62] Mørch Ý A, Donati I, Strand B L and Skjak-Braek G 2006 Effect of Ca^{2+}, Ba^{2+}, and Sr^{2+} on alginate microbeads *Biomacromolecules* **7** 1471–80
[63] Moya M L, Morley M, Khanna O, Opara E C and Brey E M 2012 Stability of alginate microbead properties *in vitro J. Mater. Sci., Mater. Med.* **23** 903–12
[64] Park M J, Choi M, Kim M and Lee D-H 2020 Injectable and cryopreservable MSC-loaded PLGA microspheres for recovery from chemically induced liver damage *Macromol. Res.* **28** 1017–25